What's the Defect? Using Mass Defects to Study Oligomerization of Membrane Proteins and Peptides in Nanodiscs with Native Mass Spectrometry

Julia A. Townsend[1], Michael T. Marty[1, *]

[1]Department of Chemistry and Biochemistry and Bio5 Institute, University of Arizona, Tucson, AZ 85721, USA

*mtmarty@arizona.edu

Abstract

Many membrane proteins form functional complexes that are either homo- or hetero-oligomeric. However, it is challenging to characterize membrane protein oligomerization in intact lipid bilayers, especially for polydisperse mixtures. Native mass spectrometry of membrane proteins and peptides inserted in lipid nanodiscs provides a unique method to study the oligomeric state distribution and lipid preferences of oligomeric assemblies. To interpret these complex spectra, we developed novel data analysis methods using macromolecular mass defect analysis. Here, we provide an overview of how mass defect analysis can be used to study oligomerization in nanodiscs, discuss potential limitations in interpretation, and explore strategies to resolve these ambiguities. Finally, we review recent work applying this technique to studying formation of antimicrobial peptide, amyloid protein, and viroporin complexes with lipid membranes.

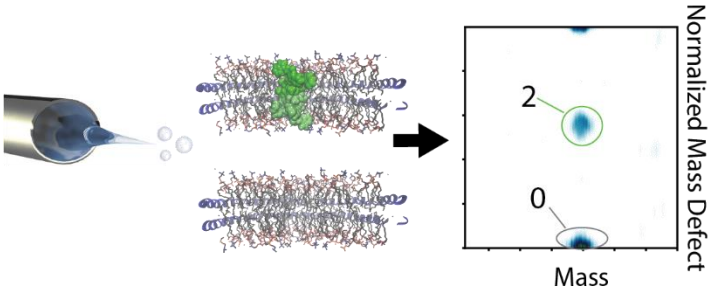

Keywords: Native mass spectrometry, nanodiscs, membrane proteins, oligomerization, mass defect analysis, lipid bilayer

1. Introduction: Oligomerization of Membrane Proteins and Peptides

Between 30–50% of proteins are thought to form oligomers.[1] Some membrane protein, such as the ATP-binding cassette transporter, TmrAB, form monodisperse and static complexes.[2, 3] Other proteins, such as the receptor tyrosine kinase family, have more dynamic interactions.[4-7] In a number of cases, their oligomerization is not well understood, such as with GPCRs.[8-10] Understanding this fundamental aspect of protein quaternary structure is important because the oligomeric state can have a significant effect on the activity of the protein.[11] For example, oligomerization of membrane proteins can affect crucial cellular functions, such as apoptosis, tumor formation, and signal transduction.[12] Similarly, membrane active peptides can oligomerize in bilayers to form functional complexes.[13] However, direct measuring the oligomeric state of membrane proteins and peptides poses a variety of analytical challenges, especially within lipid environments.[14]

Here, we will review our recent work studying the oligomerization of membrane proteins and peptides in lipid nanodiscs using native mass spectrometry (MS). We detail the data analysis methods, limitations of the technique, and strategies used to overcome these limitations. Finally, we will review the unique biophysical insights gained by applying these techniques to study viroporins, antimicrobial

peptides, and amyloid proteins. To put this new method in context, we will first briefly review common methods to study membrane protein oligomerization and discuss their strengths and limitations.

2. Methods for Measuring Membrane Protein Oligomerization

There are a variety of analytical tools that can be used for determining the oligomeric states of membrane proteins and peptides. Here, we will describe some of the most common techniques and discuss their strengths and limitations. As we examine these methods, there are three key points to consider.

First, what types of lipid environments can the technique probe? Membrane proteins can be influenced by the lipid bilayer,[15, 16] including properties like fluidity, curvature, and charge.[17, 18] Several techniques, including hydrodynamic methods, mass photometry, nuclear magnetic resonance (NMR), and native mass spectrometry (MS), generally require membrane proteins to be extracted from their native lipid environment and solubilized in a membrane mimetic, such as detergent micelles.[19, 20] Different membrane mimetics can cause varying types of interference, depending on the technique. Other techniques, including crosslinking and fluorescence methods, can be performed on proteins in diverse environments, including embedded in natural membranes.

Second, how does each technique handle polydispersity? Some techniques, like native MS, mass photometry, and hydrodynamic methods are capable of characterizing polydisperse oligomeric state distributions. Other techniques, including NMR, crosslinking, and some fluorescence methods, generally give average oligomeric state values that will be less useful for polydisperse ensembles.

Third, what is the size range for each technique? Some techniques, like native MS and fluorescence methods generally tolerate a wide range of analyte sizes, ranging from small peptides to large membrane protein complexes. Others, like mass photometry, hydrodynamic methods, and crosslinking, work better for larger proteins. Finally, NMR works best for smaller proteins and peptides and does not scale as well to larger complexes. Overall, no method is perfect, and each has tradeoffs between information content and sample tolerance.

2.1 Hydrodynamic Methods

Hydrodynamic methods like analytical ultracentrifugation (AUC) are well-established for determining the oligomeric state of soluble proteins.[21] AUC can be a powerful technique because it can effectively characterize sample polydispersity and quantify the abundance of different oligomers. However, membrane mimetics like detergent micelles are required to solubilize membrane proteins, and they can influence the size and buoyancy of membrane proteins, making interpretation of AUC data more challenging.[22] AUC can be especially challenging when the sample is polydisperse or the protein interactions are more dynamic.[23]

With size exclusion chromatography coupled with multiangle light scattering (SEC-MALS), the masses of proteins in solution can be measured through the intensity of the scattered light of a sample as it elutes from a SEC column, which also provides a retention time related to mass.[24] Like AUC, the addition of the detergent micelle can significantly interfere with both retention time of a protein from the SEC column and the way that light will scatter around the sample in solution.[25] Thus, the need for membrane mimetics can limit SEC-MALS for determining the oligomeric states of membrane proteins. Other hydrodynamic methods will face similar limitations as AUC and SEC-MALS, where the membrane

mimetic can affect the signal. In these cases, it is challenging to study smaller analytes because they contribute less to the overall size of the complex relative to the mimetic.

2.2 Mass Photometry

Mass photometry (MP) is a relatively new technique to measure the masses of biomolecules in solution. MP uses light scattering to measure the masses and relative abundances of unlabeled proteins in solution.[26] The major strength of MP is its ability to characterize polydisperse and heterogeneous samples with minimal sample consumption, broad tolerances for buffer conditions, and quick analysis.[27] However, like AUC and SEC-MALS, membrane mimetics are required and can interfere with MP analysis and interpretation.

For detergents, the strong background signal from empty micelles can overwhelm the signal from micelles with protein. To address this problem, researchers have diluted samples to below the detergent critical micelle concentration, which removes the interference. However, even with these creative approaches and use of non-interfering membrane mimetics like SMALPs and nanodiscs, interpretation still remains challenging due to the mass of the membrane mimetic.[28] Also, although oligomeric changes that cause large changes in the mass of the complex can be easily measured, MP is limited for characterizing smaller proteins and peptides due to limits in resolution and interferences from the membrane mimetic.

2.3 NMR

Nuclear magnetic resonance (NMR) spectroscopy is a powerful technique for studying the structure and dynamics of small proteins in solution as well as membrane environments. The most widely used approaches rely on many short range inter-nuclear distance measurements supplemented with angular restraints to constrain the protein to its three-dimensional fold, in part by using restraints on the distances between pairs of nuclei in the protein. However, the lack of long range restraints means that NMR is generally less useful for describing protein-protein interactions, particularly in the cases of small proteins forming homo-oligomers.[29] Relying on distance measurements alone is not straightforward in large part because it is challenging to assign restraint pairs of nuclei in the same or different polypeptide chains.[30, 31]

This limitation of distance restraints can be largely overcome in solid-state NMR studies of proteins in lipid bilayers by employing Centerband-Only Detection Of Exchange (CODEX), which is based upon anisotropic diffusion and using a label such as ^{13}C or ^{19}F.[32, 33] However, CODEX is limited for polydisperse samples and larger protein complexes.[34] Like other NMR techniques, it also needs high sample concentrations, which could drive proteins into non-physiological complexes.[35] The use of angular restraints of aligned bilayer samples[36] can also provide complementary structural information.

2.4 Chemical Crosslinking

Chemical crosslinking followed by gel electrophoresis and/or mass spectrometry is another common technique for determining the oligomeric state of proteins.[37] A major strength of crosslinking is that it can be applied while the protein is still embedded in a natural lipid bilayer by using membrane permeable crosslinkers.[38] A challenge of cross-linking experiments is that it relies on have reactive amino acid residues in the correct locations for the cross linking reaction to occur. Smaller complexes might suffer from false negatives if the right residues are not available in the right places. Also, the addition of a crosslinker can also lead to structural distortion and oligomeric artifacts, especially if too much crosslinker is added or the reaction is allowed to proceed for too long.[39, 40] Overall, the potentials for

false positives and false negatives make it challenging to confidently determine oligomeric state distributions for polydisperse ensembles from crosslinking data alone.

2.5 Fluorescence Methods

Finally, fluorescence methods can inform on the oligomeric state of a membrane protein while in the lipid bilayer.[41] FRET can be used to study dimerization by looking at distance between two labels, and fluorescence recovery after photobleaching (FRAP) provides an average diffusion constant of the protein in the lipid bilayer, which can inform on complex size. An advantage to FRAP is that it can be performed on proteins in living cells.[42] Performing the experiment in living cells adds a dimension of real-time information that none of the other techniques can provide. However, there can be major challenges with FRAP in trying to determine the diffusion coefficient of particles in the membrane, which can lead to artifacts. FRAP is also limited in its ability to resolve polydisperse samples.[43]

2.6 Native Mass Spectrometry of Membrane Proteins

Native, or nondenaturing mass spectrometry (MS) has emerged as a powerful technique for determining the oligomeric state of proteins.[44-46] Native MS uses non-denaturing sample preparation and gentle ionization to preserve the native fold of proteins in the gas phase and retain protein-protein interactions. Directly measuring the mass of the oligomeric complex usually provides a clear picture of the oligomeric states present and relative changes in the distribution.[45, 47] However, precise quantitation of the oligomeric state distribution can be challenging due to differences in ionization, transmission, and detection efficiency between ions of very different *m/z* ratios.[48, 49]

Although first applied to soluble proteins, native MS also enables the analysis of membrane proteins in a variety of membrane mimetic environments. The original and most commonly used membrane mimetic for native MS is detergent micelles.[50] When performing native MS of proteins solubilized in detergent, the entire protein-micelle complex is ionized and enters the mass spectrometer. Energy is then applied inside the mass spectrometer and labile detergent molecules are removed from the surface of the protein.[46] The removal of these detergent molecules presents the bare protein complex for mass analysis, which can then be easily interpreted like soluble proteins.

Unlike methods above, native MS uniquely allows detergents to be removed from the membrane protein complex while still preserving the oligomeric assembly for analysis. This technique is broadly applicable to complexes ranging from small membrane proteins/peptides[51] to large membrane protein assemblies.[52] However, detergent are not ideal for membrane sensitive or highly fragile complexes.[53] As reviewed by Keener *et al.*,[46] there have been a number of other membrane mimetics that have been employed for native MS, including SMALPs,[54] liposomes,[55] and nanodiscs.[56] In this review, we will discuss in detail the application of nanodiscs for determining the oligomeric state of membrane proteins with native MS.

2.7 Nanodisc Native MS

As an alternative to detergents, nanodiscs are a promising platform for the analysis of membrane proteins.[57] Nanodiscs are typically 10–13 nm bilayers, but they can be as small as 6 nm[58] and as large and 90 nm.[59] These bilayers are surrounded by a membrane scaffold protein (MSP) belt (Figure 1A). The lipid composition and size of nanodiscs can both be tuned to suit the needs of the analyte.[57, 60] Nanodiscs enable membrane proteins to be embedded in a soluble lipid bilayer.[61] Prior studies have suggested that embedding membrane proteins in nanodiscs can be more effective at preserving

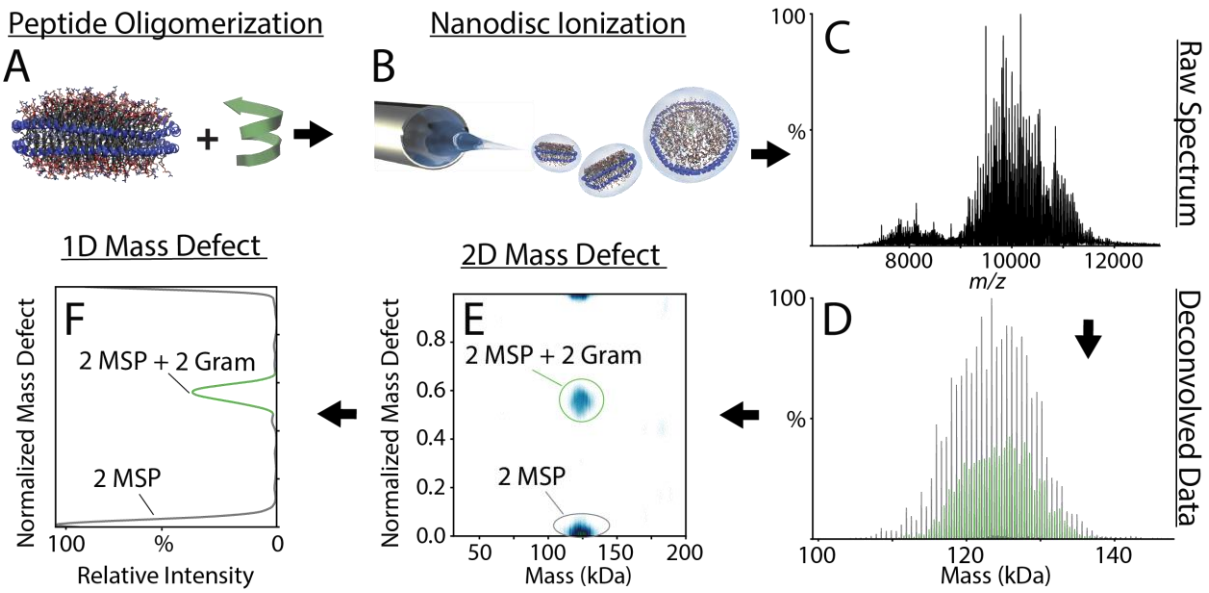

Figure 1: Schematic illustrating the experimental workflow for determining the number of peptides associated with a DMPC nanodisc. Gramicidin A (illustrated as green alpha helix) was directly added to nanodiscs (A) prior to electrospray ionization (B) for native mass spectrometry (C). The data was then deconvolved (D), and nanodiscs that contain only DMPC and MSPs are shown in grey. Nanodiscs that have two gramicidin peptides added are in green. Mass defects were calculated and are shown as a function of the overall mass of the nanodisc with specific signals labelled (E). The relative intensities of each species can be determined by summing the intensities of mass defects across all mass values (F).

membrane protein activity than detergent micelles, likely because the nanodisc bilayer more closely mimics the natural lipid bilayer.[60, 62, 63]

Over the last decade, we have worked to combine the emerging technologies of native MS and nanodiscs to enable the direct, label-free measurement of the stoichiometry of membrane proteins in an intact lipid bilayer. Native MS is gentle enough to preserve the noncovalent interactions of the entire membrane protein-nanodisc complex for mass analysis (Figure 1B),[56, 64, 65] which yields complex mass spectra of the intact nanodisc (Figure 1C). This raw data can then be deconvolved[66] to combine the multiple charge states in the *m/z* spectrum into a summed mass distribution (Figure 1D).

Nanodiscs have a series of masses due to the intrinsic heterogeneity in number of lipids per particle. For example, MSP1D1(-) nanodiscs typically contain between 140–160 1,2-dimyristoyl-*sn*-glycero-3-phosphotidylcholine (DMPC) lipids, as shown in Figure 1D.[61, 67] Because there is a polydisperse and variable number of lipids per nanodisc, it can be challenging to determine the stoichiometry of complexes embedded within the nanodisc, especially for small proteins or peptides. If we assume that the number of lipids remains constant, it is sometimes possible to infer binding stoichiometry from global shifts in the mass, such as seeing a 12 kDa shift in mass caused by binding of three 4 kDa peptides.[68] However, membrane proteins/peptides often displace lipids upon incorporation in the nanodiscs, leading to no global shift in mass and/or an uncertain number of lipids in the nanodisc.

To overcome this challenge, we developed the use macromolecular mass defect analysis to measure small shifts in mass caused by addition of proteins or peptides to the complex.[69, 70] These small shifts are independent of the total number of lipids and thus are more informative than the global mass. Here, we will present a detailed walkthrough to cover what mass defect analysis is, how mass defect analysis is performed, what it can teach us, and what we have learned from it.

3. Macromolecular Mass Defect Analysis

3.1 What is mass defect analysis?

Mass defect analysis aids in the visualization of complex mass spectra, especially when there are regular patterns of mass differences separating the peaks.[71] Our implementation of macromolecular mass defect analysis is analogous to Kendrick mass defect analysis, which is typically used in hydrocarbon analysis.[72] Mixtures of hydrocarbons often have species within the same class of molecules (such as fatty acids) that differ only in length of the chain. To help cluster classes, classic Kendrick analysis plots the mass of each hydrocarbon species relative to a repeating methylene (CH_2) unit.[73, 74] Thus, compounds that differ by any number of additional CH_2 units but are otherwise identical, cluster together.

The Kendrick mass defect is calculated by dividing the measured mass by the reference mass, classically the mass of methylene, and taking only the remainder. This remainder is the mass defect value, and it can be normalized between 0 and 1 or converted back into absolute mass by multiplying by the reference mass.[65, 70, 72, 75] Species that have exactly one additional methylene will have different integer quotients but the same remainder (mass defect). Kendrick analysis is usually visualized in two dimensions, and plots typically show the mass defect as the y-axis and the x-axis as either the integer quotient (the Kendrick mass number), the exact measured mass, or the Kendrick mass, which is a slightly corrected mass value. Although originally used in hydrocarbon analysis, Kendrick mass defect plots are also useful in clustering lipid species, and mass defect analysis in general has diverse applications in data interpretation.[76-78] Macromolecular mass defect is analogous to Kendrick mass defect, but it uses a molecule rather than methylene as the reference mass.

3.2 Mass Defect Analysis with Nanodiscs

To illustrate how macromolecular mass defect is performed and interpreted for nanodiscs, we will walk thorough an example of applying macromolecular mass defect analysis to determine the number of gramicidin A peptides embedded within an intact nanodisc (Figure 1).[70, 79] Here, we use the mass of the lipid in the nanodisc as the repeating unit reference mass.

When examining an intact nanodisc by native MS, we can generally assume that all nanodiscs contain two MSP belts, except in strange and undesirable cases.[80] For example, consider nanodiscs made up of DMPC lipids and two MSP1D1(-) belts. The mass defect value of the two MSP is determined by adding the mass of the two belts together (2 × 22,044 = 44,088 Da) and dividing it by the reference mass of DMPC (678 Da). This division yields: 44,088 Da /678 Da = 65.03. Removing the integer component of 65 gives us the normalized mass defect value of 0.03. Comparing this predicted mass defect value with the measured mass defect value (Figure 1E) confirms the number of MSP belts on the nanodisc.[69]

The mass defect can be expressed as unitless parameter (normalized to between 0 and 1), or it can be converted back into Da by multiplying by the reference mass (0.03 * 678 Da = 20 Da).[70] This

conversion tells us that nanodiscs with 2 MSP1D1(-) belts are 20 Da heavier than the nearest multiple of the DMPC lipid mass, which would be 65 * 678 Da = 44070 Da, with slight errors from rounding. Here, we will primarily discuss normalized mass defects for simplicity.

Importantly, each additional lipid changes only the integer and not the remainder of the division, so the mass defect is independent of the number of lipids in the nanodisc and informs exclusively on the number of proteins/peptides incorporated into the nanodisc.[56] Any lipids added to the 2 MSP belts to form a nanodisc will not shift the mass defect. For example, if one lipid is added, the mass will be 44,088 + 678 = 44,766 Da. Dividing by the reference mass yields: 44,766 / 678 = 66.03. Adding a lipid increases the integer component of the division (from 65 to 66), but the mass defect (0.03) remains unchanged. This principle holds for 10, 100, or 1000 bound lipids, which would change the integer to 75, 165, and 1065, respectively, but would not change the mass defect, 0.03.

3.3 Calculating Mass Defects from Native Mass Spectra

The discussion above has focused on predicting mass defect values from known masses. When applied to measured data, the same process for calculating mass defect is repeated for each deconvolved mass data point. Thus, we supplement our data of mass and intensity with a third column of mass defect. There are two typical ways that the data for macromolecular mass defect analysis can be presented, as 1D and 2D plots. With the 2D plots (Figure 1E), the data is plotted as the mass defect value (y-axis) versus the overall mass of the entire complex (x-axis). The 2D plots have the relative intensity of each species displayed in color as a heat map (z-axis).

With the 1D plots (Figure 1F), the mass defect value is plotted against the relative summed intensity from all mass data points, summing across the x-axis of the 2D plots. Ideally, each peak in the plots corresponds to a different number of oligomers associated with the nanodisc. The 1D plots more clearly reveal the global distributions of different oligomeric states, but the 2D plots preserve useful information on absolute mass that can be useful for assignments and observing shifts in the mass (discussed below). The intensities of the peaks can be extracted from the 1D and 2D plots and averaged over replicates. These average intensities can then be plotted in a grid or bar chart for different oligomeric states and under different conditions to gain insight on trends and specificities across species and lipid types (see below).

The approach described above relies on first deconvolving the data from *m/z* into mass. However, it is possible to use the phase information in a Fourier transformed *m/z* spectrum to reconstruct a macromolecular mass defect trace.[72] Although it is only currently possible to get phase information from the entire spectrum to assemble a 1D plot, it may be possible to create similar 2D plots with a Gabor transform.[81] Excitingly, there is excellent agreement between mass defect profiles measured with direct Fourier methods and with deconvolved data.[72]

3.4 Measuring Association of Biomolecules to Nanodiscs

Because the lipids do not affect the mass defect, the mass defect value reflects the mass of the non-lipid species incorporated into the nanodisc. Thus, after we know the mass defect shift caused by the MSP belts, we can examine additional shifts to measure association of other biomolecules. For example, by adding antimicrobial peptides (AMPs) to nanodiscs, we can measure the stoichiometries of peptides associating with nanodiscs using mass defect analysis (Figure 1).[75, 82, 83] After the raw mass spectra are deconvolved, the normalized mass defect values are compared against predicted values to reveal the different stoichiometries associated with the nanodisc (Figure 1E and F).

For example, based on the mass of gramicidin A (GA, 1882.3 Da), we can calculate the mass defect value for each possible stoichiometry in the nanodisc (shown in Table 1). Because all nanodiscs have two MSP belts, we calculate the predicted mass defect by adding the mass of GA to the mass of the two MSP belts and dividing it by the lipid mass. For example, a DMPC nanodisc containing 4 GA peptides would be determined by: (44,088 + (1882.3 × 4)) / 678 = 76.13. The mass defect value is the remainder value of this division, so the mass defect value for 4 GA peptides in a DMPC nanodisc would be 0.13, as shown in Table 1.

Table 1: The expected mass defect values for gramicidin A in nanodiscs with MSP1D1(-) belts comprised of DMPG and DMPC lipids.

Stoichiometry	DMPG (667 Da)	DMPC (678 Da)
0	0.09	0.03
1	0.92	0.80
2	0.74	0.58
3	0.57	0.36
4	0.39	0.13
5	0.21	0.91
6	0.03	0.68
7	0.85	0.46
8	0.68	0.24
9	0.50	0.01
10	0.32	0.79

Mass defects for oligomeric complexes can also be calculated by combing individual mass defects with a form of modular arithmetic. Addition and multiplication of mass defects follow standard arithmetic except that the integer part is subtracted (or added, as shown in the next paragraph) to reset the mass defect between 0 and 1. Thus, mass defect arithmetic will "wrap around" to stay within the 0 to 1 window. For example, gramicidin A has a mass defect of 0.78 (1882.3 / 678 = 2.78 = 0.78) in DMPC. As shown above, 2×MSP1D1(-) has a mass defect of 0.03. Thus, a GA monomer in nanodiscs will be 0.03 + 0.78 = 0.81. Two GA in nanodiscs will be 0.03 + 2 × 0.78 = 1.59, but the integer is dropped to yield simply 0.59. Adding another GA monomer to calculate three GA in nanodiscs will yield 0.59 + 0.78 = 1.37, which wraps around again to yield 0.37. Numbers are only slightly different from Table 1 due to rounding.

We can use this modular wrapping for convenience in calculations. For example, we could view a mass defect of 0.78 as equivalent to –1 + 0.78 = –0.22, wrapping it down to a window of –1 to 0. Here, two GA in nanodiscs would be calculated by taking the mass defect of the monomer and subtracting 0.22: 0.81 – 0.22 = 0.59. For any negative values calculated this way, we simply need to add enough integers to get the value within 0 to 1. For example, monomeric GA in nanodiscs could be calculated by 0.03 – 0.22 = –0.19 + 1 = 0.81. In fact, we can choose any convenient window for normalized mass defects, provided it has a width of 1. It is sometimes useful to wrap to a window of –0.5 to 0.5. Thus, mass defects can be combined in useful and predictable ways.

We can compare these predicted mass defect values of each stoichiometry to measured shifts in the mass defect plots to determine the number of proteins or peptides associated with the nanodisc. In Figure 1, clear signals are observed for 0 GA (mass defect of 0.03) and 2 GA (mass defect of 0.58) per nanodisc. It is not uncommon that measured mass defect values will be slightly higher than predicted due to adduction or incomplete desolvation.

The distributions of stoichiometries provide important information on the oligomeric specificities of membrane proteins/peptides. As shown in Figure 1, there is a clear signal for 0 and 2 GA per nanodisc, but not for 1 and 3. If GA incorporated as only monomers or nonspecific complexes, it should show a roughly Poisson distribution of stoichiometries. Because only even stoichiometries are observed, this peptide incorporates preferentially in units of 2. However, the distribution of dimers is roughly Poisson, which indicates that specific higher order tetramer or hexamer complexes are not preferred under these conditions.[75] Instead, these nanodiscs likely accommodate multiple dimers that lack specific inter-dimer interactions. Examining the distributions of different species present with mass defect analysis can thus reveal specific complex formation, as described with examples below.

4. Ambiguities and Work Arounds

Although macromolecular mass defect analysis can be a powerful technique for determining the oligomeric states of membrane proteins and peptides in nanodiscs, it also has limitations. The primary limitation is that some combinations of protein/peptide mass and lipid reference mass yield mass defect values of different oligomers that are very similar, making it challenging to assign the stoichiometry. In the most extreme case, where the mass defect of the monomer is exactly 0, the protein/peptide mass is equal to an integer number of lipids. Thus, each oligomer would be indistinguishable from lipids or from one another, making it impossible to assign a given peak to stoichiometries from mass defect alone. Anytime when mass defects are close to 0, ambiguous overlaps will occur.

In a less extreme case, when daptomycin, a cyclic lipopeptide antibiotic,[84, 85] is added to nanodiscs made up of 1,2-dipalmitoyl-sn-glycero-3-phosphocholine (DPPC) lipids, there is near overlap of several stoichiometries, including the mass defects for 0 and 5, 1 and 6, 2 and 7, and 3 and 8 (shown in gray dashed lines in Figure 2A and 2C). This near overlap makes it challenging to confidently assign the stoichiometry of the peptide inside the nanodisc from a single spectrum.

For example, the mass defect for a DPPC nanodisc with one daptomycin incorporated is determined by the remainder after dividing the mass of the two MSP belts plus the one daptomycin (1,619.7 Da) by the reference mass, or (44,088 Da + 1,619.7 Da)/734 Da = 62.27. The mass defect value of 0.27 is similar to the mass defect value for six

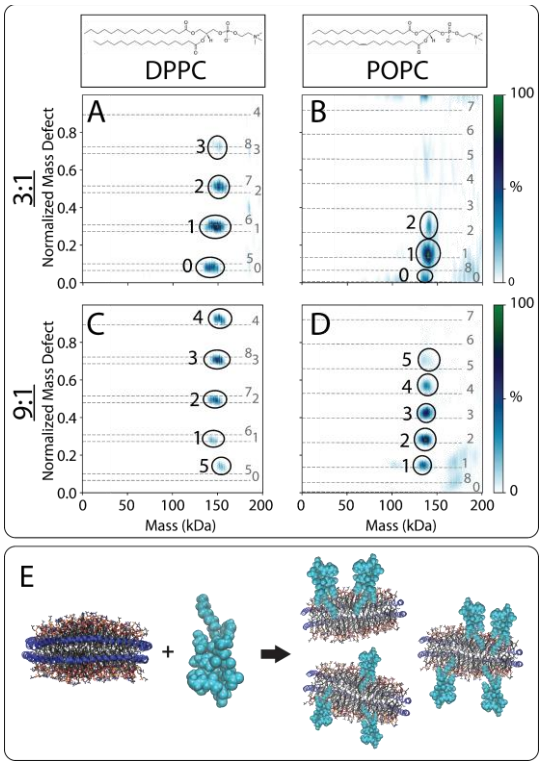

Figure 2: Mass defect heatmaps of daptomycin incorporated into DPPC nanodiscs (A, C) and POPC nanodiscs (B, D) at ratios of 3 daptomycin per nanodisc (A, B) and 9 daptomycin per nanodisc (C, D). The possible stoichiometries based on the mass defect values are annotated in dashed gray lines, and the assigned stoichiometries are circled in black on each heatmap (A-D). Panel E illustrates the possible incorporation of daptomycin into nanodiscs.

daptomycin incorporated into the same nanodisc, which is (44,088 + 1619.7*6)/734 = 73.30 or 0.30. This difference in mass defect of 0.03 corresponds to an absolute mass difference of 22 Da, which is not possible to resolve with assemblies this large and complex.

To reframe these calculations, the mass defect daptomycin alone (no MSP belts) is 1,619.7/734 = 0.207. A stoichiometry of 5 daptomycin molecules will have a mass defect of 5 × 0.207 = 0.03. Thus, any stoichiometries that differ by 5 are only 0.03 apart in mass defect, which is impossible to distinguish in practice. In general, combinations of protein/peptide and reference masses that yield mass defects close to simple fractions (1/2, 2/3, 1/4, etc.) will be prone to overlap. In this example, the proximity of the mass defect to 1/5 (0.2) causes stoichiometries that differ by 5 to be similar.

Due to these ambiguities in assignment, we cannot tell from this spectrum alone whether the distribution in Figure 2C should be assigned as sets of [0, 1, 2, 3], [5, 6, 7, 8], or some mixture of these assignment sets. However, several strategies can be used to help disambiguate these assignments.

4.1 Strategies for Disambiguating Mass Defect Assignments

Strategy 1: Leverage Statistics. The first strategy for disambiguation is to carefully examine the statistical distribution. If we can make assumptions about the distribution, like assuming a Poisson distribution, we can exclude assignments that do not fit the distribution. For example, in Figure 2A, the distribution fits a roughly Poisson distribution for [0, 1, 2, 3]. However, a distribution of [5, 6, 7, 8] is lacking key intensity for 4 that would be expected. Thus, we can infer that [0, 1, 2, 3] is the more likely assignment set. However, not all systems show obvious statistical distributions, as described below. Thus, this strategy relies on our ability to make assumptions about the statistical distribution, which often requires comparison of multiple spectra.

Strategy 2: Compare Spectra Across Different Conditions. Another useful strategy for disambiguation is to look at sets of spectra rather than an individual spectrum. For example, we can assume that distributions will shift to higher stoichiometries at higher concentrations of added peptide/protein. We can thus rule out any distributions that do not fit logically. For example, if we assign the 9:1 ratio of peptide:nanodisc in Figure 2C as [1, 2, 3, 4, 5], the more dilute peptides in Figure 2A at the 3:1 ratio are more likely to be [0, 1, 2, 3] than [5, 6, 7, 8]. We can also rule out stoichiometries that do not make sense considering the global ratios. For example, a larger set of [10, 11, 12, 13] would have similar mass defect values to [0, 1, 2, 3], but it is impossible to have this larger set of stoichiometries if the global ratio is only 3:1 peptide:nanodisc.

Similarly, we have previously used collisional activation inside the mass spectrometer as a way to help disambiguate spectra.[75, 86] Collisional activation is a technique where voltages are increased inside the mass spectrometer to increase the speed that the analyte collides with inert gas molecules inside the instrument. Collisional activation can eject molecules from the nanodiscs.[65, 87] With peptide nanodiscs, we can perform collisional activation to eject some of the peptides from the nanodisc. Shifting the distribution down to lower stoichiometries with ejection has similar value as shifting the distribution up by adding more peptide. Because Poisson distributions will distort as they approach zero (described in Strategy 1), activation can help determine the stoichiometry of peptides in the nanodisc by breaking the symmetry of the distribution. However, not all systems eject efficiently and predictably with collisional activation. For example, many membrane proteins break off the MSP belt rather than eject protein subunits.[69]

Strategy 3: Look for Spectral Shifts. If we see clear shifts in the absolute mass of the nanodisc, we can use these to aid in disambiguation. For example, in Figure 2A and 2C, we can see that each additional daptomycin molecule shifts the mass slightly higher. Thus, in Figure 2C, the 0 and 5 state could each be populated based on the distribution (Strategy 1) and on comparisons with a broader data set (Strategy 2), but the slight increase in mass over the neighboring state with 1 incorporated suggest that 5 is more likely.

However, not all peptides show a clear mass shift upon incorporation. Many, like α-syn shown below in Figure 5C, do not shift the overall mass of the nanodisc upon incorporation, likely because the same mass of lipids is displaced upon addition of the protein/peptide mass to the bilayer.[88]

Strategy 4: Change the Reference Mass. Similar to Strategy 2, a different lipid with a different reference mass can be used to disambiguate assignments.[70, 75] As shown in Figure 2B and 2D, using 1-palmitoyl-2-oleoyl-*sn*-glycero-3-phosphocholine (POPC) lipids in the nanodisc shifts the possible mass defect values so that they are no longer ambiguous. For example, with one daptomycin incorporated into a POPC nanodisc, the mass defect value is 0.41, which is determined by (44,088 + 1619.7 Da)/760.1 Da = 60.13 for a mass defect of 0.13. This value is now considerably different from the mass defect value for six daptomycin incorporated into a DMPC nanodisc, which is 0.78. The use of different lipids can be a powerful tool for disambiguating the assignments for mass defect analysis.

One major challenge associated with using different lipids to aid in the assignment of mass defect values is that this strategy relies on the protein behaving identically in both lipid conditions. This assumption can pose issues as some proteins will take on markedly different oligomeric states in different lipid environments, as shown in Figure 3 and Figure 4.[75, 82, 83, 89]

Strategy 5: Change the Protein/Peptide. If changing the lipid reference changes the oligomeric state distribution, the mass of the protein or peptide must be changed instead. It is important that these changes result in mass shifts great enough to alter the mass defect values without perturbing the natural oligomeric state of the protein. This could be done by creating proteins that are labeled with stable isotopes, such as ^{15}N.[90] Another way that the mass of the protein could be slightly shifted is through the addition of one or two amino acids to the protein by genetic engineering in sites that do not affect the structure or function.[69] Both methods are useful for disambiguating the oligomeric states of proteins with mass defect analysis.

4.2 Additional Challenges and Considerations

Another limitation of mass defect analysis is that it provides little structural information on the proteins inside of the nanodisc. Mass defect analysis can only inform on the number of proteins or peptide incorporated into the bilayer, not the orientation of these molecules (Figure 2E). However, mass defect analysis can be done alongside other experiments that can provide structural information on the oligomeric state and the solvent exposed regions of the protein, such as hydrogen-deuterium exchange MS or fast photochemical oxidation of protein (FPOP).[91, 92] The combination of mass defect analysis with footprinting can provide a depth of information on the structure, lipid specificities, and protein-protein interactions of membrane proteins.[93]

Another challenge in macromolecular mass defect analysis is that the mass spectra for this data can sometimes be noisy and challenging to resolve. It is important with mass defect analysis of nanodiscs that all components of the nanodisc are free of impurities and adductions. We have found

that common sources of impurities are the lipids used or the membrane protein embedded within the nanodisc. These impurities can be identified more easily if there is upstream characterization of these materials prior to nanodisc assembly. We typically characterize membrane proteins with native MS in detergent prior to nanodisc assembly to confirm the purity and mass. We also create control nanodiscs with no membrane protein embedded to ensure that there are not any contaminants present in the lipids that could interfere with the mass defect analysis. For example, with pIAPP, a low-level contaminant was present in all samples that was disregarded due to its presence in the control.[94]

Another challenge with mass defect analysis can be the loss of labile interactions. Although native MS is gentle enough to preserve noncovalent interactions, fragile interactions are sometimes disrupted inside the instrument. These disruptions can also affect mass defect analysis results. For example, daptomycin showed lower incorporation in 1,2-dimyristoyl-*sn*-glycero-3-phosphoglycerol (DMPG) lipid bilayers by native MS and mass defect analysis, but FPOP analysis clearly showed similar membrane association to DMPC. Our interpretation was that the interactions are relatively weak and do not survive native MS analysis.[93] Fragile interactions can be better preserved for native MS by using low concentrations of charge manipulation reagents. Previous work has revealed that charge reducing agents, such as imidazole, triethylammonium acetate, and trimethyl amine oxide, can be useful for preserving noncovalent interactions inside the mass spectrometer.[75, 95-97]

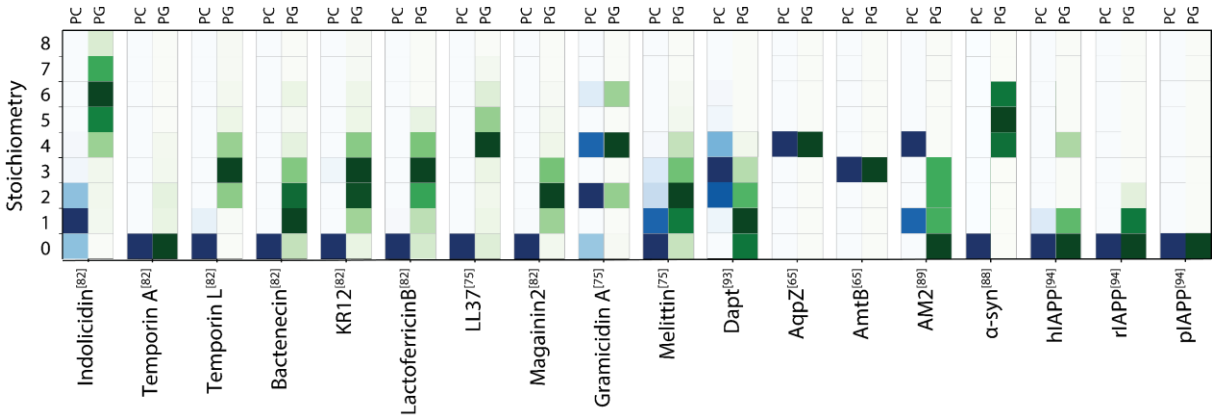

Figure 3: The abundances (shown by color density) of different stoichiometries of different peptides and proteins incorporated into nanodiscs made of PC (*blue*) and PG lipids (*green*), characterized with native MS of peptide or protein-nanodisc complexes. The abundances of the proteins and peptides were obtained by averaging the extracting the normalized mass defect values for each stoichiometry. All molecules (except proteins AqpZ, AmtB, and AM2) were added at a ratio of 9:1 peptide to nanodisc. Superscripts next to protein/peptide name indicate reference number. Data for the PC lipid conditions for rIAPP and pIAPP is unpublished.

5. Applications of Mass Defect Analysis with Nanodiscs

Over the last several years, macromolecular mass defect analysis has been used to characterize both the oligomeric and lipid specificities of a variety of biomolecules, including AMPs, amyloid proteins, viroporins, and larger membrane protein complexes. Lipid specificity can be determined by comparing the association of proteins/peptides into nanodiscs containing different lipids. Either the total levels of association[82, 93] or the specific distributions[83] can be compared to explore how lipid head groups and tails affect protein/peptide association with the nanodisc bilayer.

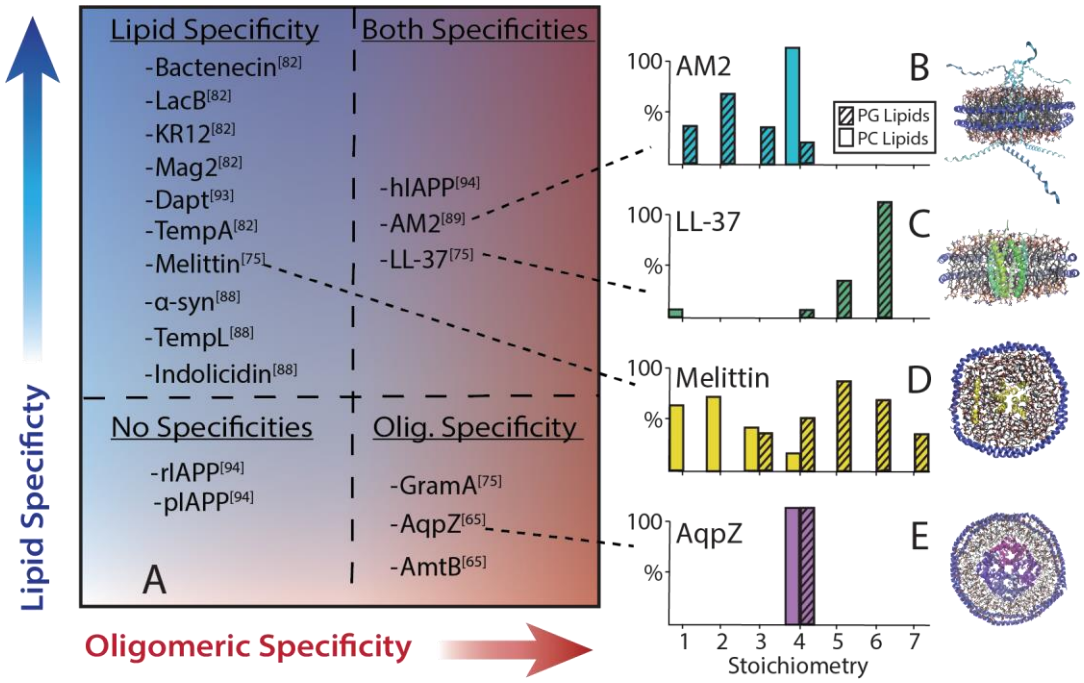

Figure 4: Schematic illustrating the variations in stoichiometry and lipid specificities of biomolecules characterized through mass defect analysis (A). Parts B, C, D, and E highlight some examples of different biomolecules shown. (B) AM2, a viroporin, showed high levels of oligomeric specificity in some lipids and little specificity in other lipid conditions. (C) LL-37, an AMP, only incorporated in phosphatidylglycerol (PG) nanodiscs and appeared to have some oligomeric specificity. (D) Melittin, another AMP, had no oligomeric specificity but incorporated into PG lipids at higher levels than phosphatidylcholine (PC) lipids. (E) AqpZ, a tetrameric membrane protein, had high oligomeric specificity but no lipid preferences. Superscripts next to protein/peptide name indicate reference number.

Although mass defect analysis only directly measures the stoichiometry of membrane protein/peptides associated with the nanodisc, examining the statistical distribution of stoichiometries can reveal whether the proteins associating with the nanodisc are forming specific oligomeric complexes or are simply randomly associating with the nanodisc. Proteins/peptides that interact nonspecifically with the nanodisc, either by associating as monomers or by forming nonspecific oligomeric complexes, exhibit a roughly Poisson distribution of stoichiometries that increases with higher concentrations. In contrast, proteins/peptides that form specific complexes exhibit a non-Poisson distribution, such as the GA peptide in Figure 1.[75] Our experiments have discovered a wide range of behaviors for these complexes, as shown in Figure 3 and Figure 4. We will begin by discussing examples of highly specific oligomeric complexes before continuing to nonspecific complexes and closing with systems that show partial specificity.

5.1 Specific Membrane Protein Complexes

Highly specific oligomeric complexes may show only a single oligomeric state within the nanodiscs, which we observed with several stable membrane protein complexes. These specific

oligomers tend to have minimal lipid specificities, forming the same oligomer in different lipid environments. For example, the membrane protein aquaporin Z (AqpZ) had exactly four monomers per nanodisc (Figure 4E), which indicates highly specific tetramers, consistent with known structures.[98, 99] AqpZ incorporated as only tetramers in bilayers of either PC or PG lipids, demonstrating no lipid preferences.[65] Similar results were seen for AmtB, which formed monodisperse trimers in both lipid environments. Gram A, discussed above, was also largely lipid insensitive, and although multiple dimers could incorporate into a single nanodiscs, we only saw evidence for specific dimer complexes.[75]

5.2 Non-specific Peptide Complexes

In contrast with highly specific membrane proteins, many antimicrobial peptides had nearly Poisson distributions that indicated nonspecific association with the nanodiscs. For example, melittin did not assemble specific complexes, as shown in Figure 4D.[75] However, melittin incorporated into PG bilayers at higher stoichiometries than PC bilayers, showing clear lipid specificity. The tendency of AMPs to show some preference for more anionic PG lipids over zwitterionic PC lipids but little oligomeric specificity was common across many of the AMPs studied (Figure 3 and Figure 4).[75, 82, 83] This trend may provide insight to the mechanisms of action for AMPs, suggesting that AMPs target the anionic bacterial membranes but generally do not need to form specific oligomers to have antimicrobial effects.[100, 101]

Mass defect analysis was also able to reveal the oligomeric states and lipid specificities of α-synuclein (α-syn), as shown in Figure 3 and Figure 5. We discovered that α-syn incorporated in stoichiometries up to five α-syn per nanodiscs and preferred PG lipids.[88] However, no specific α-syn oligomers were detected. Similar results were observed for rat islet amyloid polypeptide.[94]

5.3 More Complicated Oligomerization

Between the two extremes of highly specific and nonspecific, several systems had more complex oligomeric behaviors. Unlike most other AMPs, LL-37 tended to associate with nanodiscs with a greater degree of oligomeric specificity, associating preferentially in units of six that indicate preference for hexamer. LL-37 had significant lipid specificity and only incorporated in appreciable numbers into PG bilayers (Figure 3 and Figure 4C). Interestingly, LL-37 showed lipid tail dependence in how it assembled complexes, preferring dimer intermediates in DMPG and trimer intermediates in DPPG. FPOP also revealed tail-dependent membrane interactions of LL-37.[68] Overall, the preference of LL-37 for hexamers with dimer or trimer intermediates was unique and complex.

Another unusual example of lipid and oligomeric specificity is the case of viroporin M2 from influenza A (Figure 4B). In DMPG lipids, there was a roughly Poisson distribution of stoichiometries measured, ranging from one to four AM2 associated with the nanodisc. This statistical distribution of species suggests that there is likely no specific complex formation for AM2 in these PG lipids. Similarly, when added to DMPC lipids, there also appeared to be a Poisson distribution of AM2 incorporation. However, when embedded in DPPC lipids, which form a thicker bilayer, AM2 only incorporated in units of four and one (Figure 3, 4B, and 6A). The specificity for units of four suggests that AM2 may be forming a specific tetramer complex in the DPPC lipids.[89] These differences in incorporation among lipid types suggest that bilayer thickness may affect complex formation.[102]

These applications of mass defect analysis reveal a wide range of behaviors that peptides and proteins exhibit when associated with nanodiscs. Figure 3 and Figure 4 provide an overview of most of the proteins and peptides analyzed with nanodisc mass defect analysis to date. Some proteins and peptides appear to self-assemble into highly specific oligomers regardless of the types of lipids they are

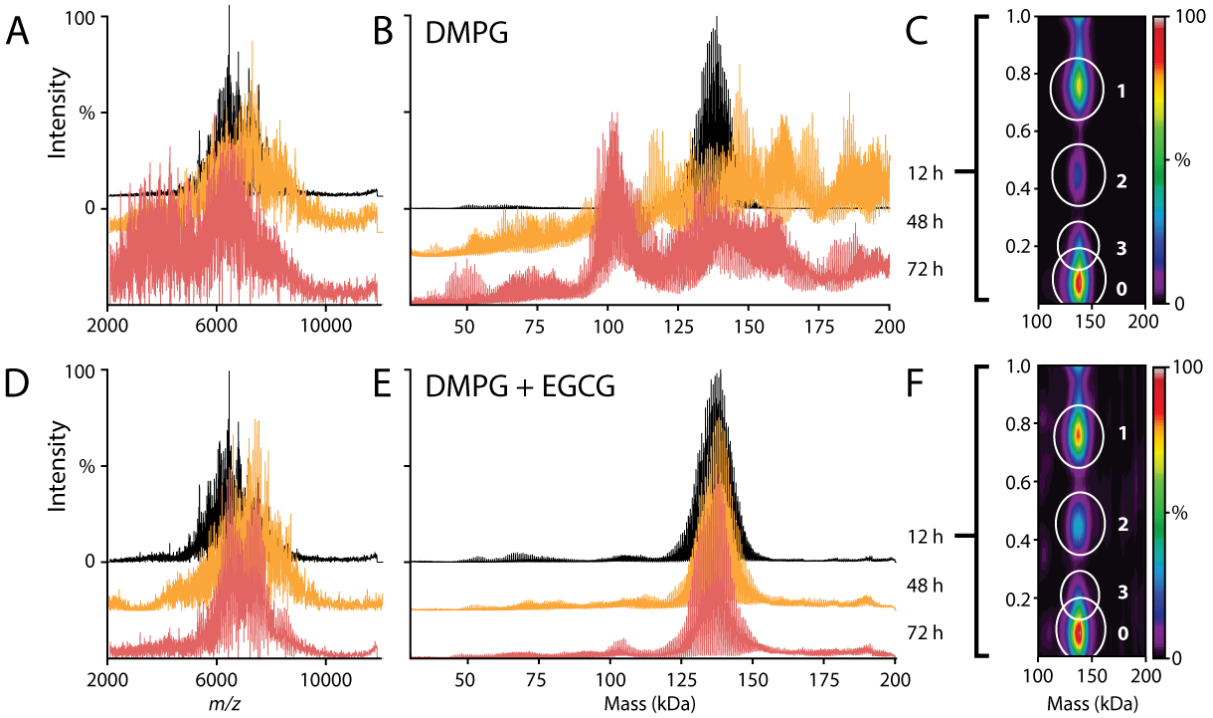

Figure 5: Native mass spectra of α-syn:DMPG nanodiscs that have been incubated for 12 h (*black*) 48 h (*orange*) and 72 h (*red*). The raw (A) and deconvolved (B) mass spectra suggest a disruption of the nanodisc by 48 h without the addition of EGCG. The 2D mass defect plot (C) indicates the association of up to 3 α-syn to the nanodisc at 12 h, prior to nanodisc disruption. With the EGCG, the raw (D) and deconvolved (E) mass spectra reveal that the nanodisc has remained intact. The 2D mass defect plot (F) shows the association of up to 3 α-syn into the nanodiscs, nearly identical to (C) without EGCG. Figure reproduced with permission from Sanders, H.M., Kostelic, M.M., Zak, C.K., and Marty, M.T. Lipids and EGCG Affect α-Synuclein Association and Disruption of Nanodiscs. *Biochem.* **2022** 61 (11), 1014-1021. Copyright 2023 American Chemical Society.

surrounded with, such as AqpZ, AmtB, and Gramicidin A. Conversely, other biomolecules exhibited little oligomeric specificity but had significant preference for certain lipid environments, such as Bactenecin and LacB. Others, like LL-37 and AM2 had more complex behaviors. Thus, mass defect analysis can be a powerful technique for characterizing the oligomerization of membrane-bound molecules.

5.4 Measuring Drug Binding and Effects

Beyond determining the stoichiometries of proteins in nanodiscs, mass defect analysis can also reveal how small molecules affect membrane interactions. For example, we used mass defect analysis to study the influence of small molecule (−)-epigallocatechin 3-gallate (EGCG) on α-syn in nanodiscs.[88] EGCG is a flavonoid found in green teas that inhibits the formation of amyloid fibrils.[103, 104] When adding α-syn to a DMPG nanodisc for 48 h or greater, the nanodiscs were significantly disrupted, as indicated by the unresolvable spectra (Figure 5A and B). However, when EGCG was added in addition to the α-syn and DMPG nanodiscs, the nanodisc remained intact (Figure 5D and E). Interestingly, mass defect analysis revealed that, at 12 h or less, samples with and without EGCG had the same amount of α-syn associated with the nanodisc (Figure 5C and F). The striking similarities suggest that the addition of EGCG prevents lipid bilayer disruption in nanodiscs that contain α-syn, but it does not prevent the initial association of α-syn with the nanodisc.

Finally, mass defect can also be used to detect drug binding to membrane protein complexes in intact nanodiscs by detecting small shifts in the mass of the assembly. In DPPC nanodiscs, AM2 assembled into stoichiometries of one and four, as described above and shown in Figure 6A. Amantadine (AMT) specifically binds to the AM2 tetramer,[105, 106] but prior research had suggested the possibility of either one or four AMT molecules binding per tetramer complex.[107, 108] After adding 40 µM AMT to AM2 nanodiscs with DPPC lipids, we measured shifts in the mass defect heat map that corresponded to the binding of AMT to the AM2 tetramer but not the monomer (Figure 6B). We were also able to resolve the stoichiometry of drug binding, measuring both one and four amantadine bound to the tetrameric M2. Adding higher concentrations of AMT increased in the intensity of the tetramer with four AMT bound (Figure 6C). These exciting results show how mass defect analysis can be applied to characterize the relationships between the small molecules that may interact with proteins and lipid bilayers.

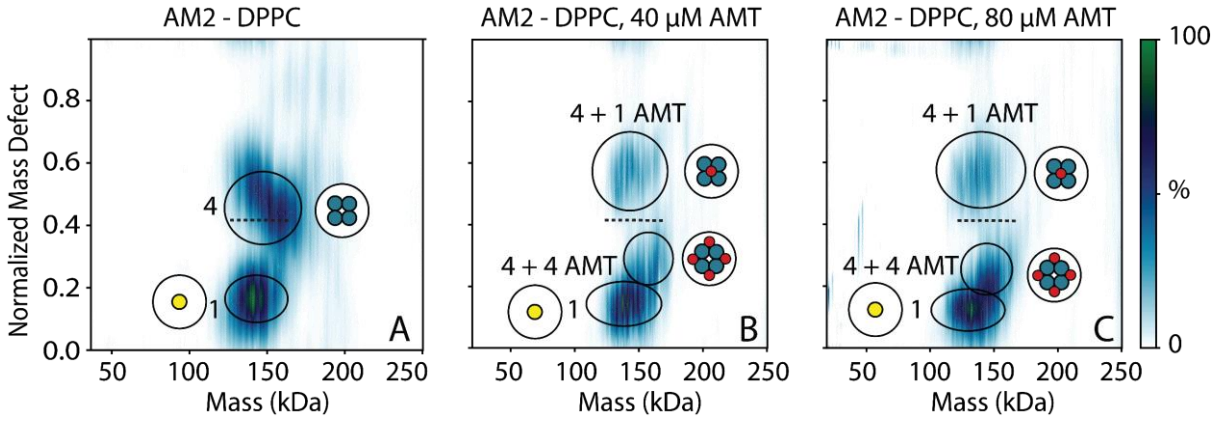

Figure 6: Mass defect heat maps of AM2 in DPPC nanodiscs (A) with 40 µM amantadine added (B) and 80 µM amantadine (AMT) added (C). The dashed line indicates the shift in the tetramer upon the binding of AMT. Figure adapted with permission from Townsend et al, Influenza AM2 Channel Oligomerization Is Sensitive to Its Chemical Environment. Anal Chem. **2021,** 93(48): 16273-16281. Copyright 2023 American Chemical Society.

6. Outlook and Future Directions

The increasing prevalence of high-resolution mass spectrometry has enabled the analysis of increasingly heterogenous assemblies. Macromolecular mass defect analysis aids in the visualization and analysis of these complex mass spectra. There is a wide range of future applications for macromolecular mass defect analysis, including analyzing data of polymer-conjugated proteins[109] and proteins with complex glycosylation patterns.[110, 111] Here, an individual glycan unit such as a mannose can be used as the reference mass. All glycoforms that differ only in mannose units will cluster together. Similarly, the monomer mass could be used as the reference in polymer spectra to explore modifications to the chain.

Macromolecular mass defect analysis is also useful to visualize binding to oligomeric complexes. If the protein monomer mass is used as the reference mass, everything that differs only in the number of protein monomers will cluster together, giving distinct clusters for ligand or adduct binding. This approach may be powerful for characterizing drug binding to proteins and can provide information on which oligomers bind the drug. In general, macromolecular mass defect analysis can be effective for

visualizing any complex spectra where it is useful to cluster things that differ by a specific reference mass.

7. Conclusions

Macromolecular mass defect analysis provides an effective bridge to combine the unique technologies of native mass spectrometry and nanodiscs. Mass defect analysis enables direct, label-free measurement of oligomerization of proteins and peptides in lipid nanodiscs. By combining these technologies, we can characterize the patterns of oligomeric and lipid specificities of a wide range of peptides and proteins, as well as characterizing the influence of small molecules on proteins and nanodiscs. Our hope is that this article provides a foundation for others to both use and interpret mass defect data, inspiring new applications to understand complex biophysical interactions.

8. Acknowledgements

The authors thank NIH/NIGMS for funding through R35 GM128624 to M.T.M. and T32 GM008804 to J.A.T., who was also funded by the ACS DAC, and ARCS fellowships. The authors thank all members of the Marty Lab who have worked on these projects and other, especially Dr. Deseree Reid, Dr. Larry Walker, and Dr. Henry Sanders, as well as collaborators, especially Prof. Martin Zanni, Prof. Jun Wang, and Prof. Stan Opella.

Abbreviations:

Mass spectrometry (MS), analytical ultra centrifugation (AUC), size exclusion chromatography coupled with multiangle light scattering (SEC-MALS), mass photometry (MP), centerband-only detection of exchange (CODEX), fluorescence recovery after photobleaching (FRAP), 1,2-dimyristoyl-*sn*-glycero-3-phosphotidylcholine (DMPC), membrane scaffold protein (MSP), antimicrobial peptides (AMP), gramicidin A (GA), 1,2-dipalmitoyl-sn-glycero-3-phosphocholine (DPPC), 1-palmitoyl-2-oleoyl-*sn*-glycero-3-phosphocholine (POPC), fast photochemical oxidation of protein (FPOP), 1,2-dimyristoyl-*sn*-glycero-3-phosphoglycerol (DMPG), aquaporin Z (AqpZ), α-synuclein (α-syn), (−)-epigallocatechin 3-gallate (EGCG), amantadine (AMT)

9. References

1. Frieden, C., Protein oligomerization as a metabolic control mechanism: Application to apoE. *Protein Sci* **2019,** *28* (4), 837-842.
2. Kim, J.; Wu, S.; Tomasiak, T. M.; Mergel, C.; Winter, M. B.; Stiller, S. B.; Robles-Colmanares, Y.; Stroud, R. M.; Tampé, R.; Craik, C. S.; Cheng, Y., Subnanometre-resolution electron cryomicroscopy structure of a heterodimeric ABC exporter. *Nature* **2015,** *517* (7534), 396-400.
3. Nöll, A.; Thomas, C.; Herbring, V.; Zollmann, T.; Barth, K.; Mehdipour, A. R.; Tomasiak, T. M.; Brüchert, S.; Joseph, B.; Abele, R.; Oliéric, V.; Wang, M.; Diederichs, K.; Hummer, G.; Stroud, R. M.; Pos, K. M.; Tampé, R., Crystal structure and mechanistic basis of a functional homolog of the antigen transporter TAP. *Proceedings of the National Academy of Sciences* **2017,** *114* (4), E438-E447.
4. Nooren, I. M. A.; Thornton, J. M., Structural Characterisation and Functional Significance of Transient Protein–Protein Interactions. *Journal of Molecular Biology* **2003,** *325* (5), 991-1018.
5. Acuner Ozbabacan, S. E.; Engin, H. B.; Gursoy, A.; Keskin, O., Transient protein–protein interactions. *Protein Engineering, Design and Selection* **2011,** *24* (9), 635-648.

6. Šachl, R.; Čujová, S.; Singh, V.; Riegerová, P.; Kapusta, P.; Müller, H.-M.; Steringer, J. P.; Hof, M.; Nickel, W., Functional Assay to Correlate Protein Oligomerization States with Membrane Pore Formation. *Analytical Chemistry* **2020,** *92* (22), 14861-14866.
7. Chung, I., Optical measurement of receptor tyrosine kinase oligomerization on live cells. *Biochim Biophys Acta Biomembr* **2017,** *1859* (9 Pt A), 1436-1444.
8. Park, P. S.; Filipek, S.; Wells, J. W.; Palczewski, K., Oligomerization of G protein-coupled receptors: past, present, and future. *Biochemistry* **2004,** *43* (50), 15643-56.
9. Palczewski, K., Oligomeric forms of G protein-coupled receptors (GPCRs). *Trends Biochem Sci* **2010,** *35* (11), 595-600.
10. Sleno, R.; Hébert, T. E., The Dynamics of GPCR Oligomerization and Their Functional Consequences. *Int Rev Cell Mol Biol* **2018,** *338*, 141-171.
11. Hashimoto, K.; Panchenko, A. R., Mechanisms of protein oligomerization, the critical role of insertions and deletions in maintaining different oligomeric states. *Proceedings of the National Academy of Sciences* **2010,** *107* (47), 20352-20357.
12. Xie, X.; Cheng, Y.-S.; Wen, M.-H.; Calindi, A.; Yang, K.; Chiu, C.-W.; Chen, T.-Y., Quantifying the Oligomeric States of Membrane Proteins in Cells through Super-Resolution Localizations. *The Journal of Physical Chemistry B* **2018,** *122* (46), 10496-10504.
13. Avci, F. G.; Akbulut, B. S.; Ozkirimli, E., Membrane Active Peptides and Their Biophysical Characterization. *Biomolecules* **2018,** *8* (3).
14. Helbig, A. O.; Heck, A. J.; Slijper, M., Exploring the membrane proteome--challenges and analytical strategies. *J Proteomics* **2010,** *73* (5), 868-78.
15. Jiang, Y.; Thienpont, B.; Sapuru, V.; Hite, R. K.; Dittman, J. S.; Sturgis, J. N.; Scheuring, S., Membrane-mediated protein interactions drive membrane protein organization. *Nature Communications* **2022,** *13* (1), 7373.
16. Pal, S.; Chakraborty, H.; Chattopadhyay, A., Lipid Headgroup Charge Controls Melittin Oligomerization in Membranes: Implications in Membrane Lysis. *The Journal of Physical Chemistry B* **2021,** *125* (30), 8450-8459.
17. Bagheri, Y.; Ali, A. A.; You, M., Current Methods for Detecting Cell Membrane Transient Interactions. *Frontiers in Chemistry* **2020,** *8*.
18. Brown, M. F., Curvature forces in membrane lipid-protein interactions. *Biochemistry* **2012,** *51* (49), 9782-95.
19. Orwick-Rydmark, M.; Arnold, T.; Linke, D., The Use of Detergents to Purify Membrane Proteins. *Curr Protoc Protein Sci* **2016,** *84*, 4.8.1-4.8.35.
20. Kermani, A. A., A guide to membrane protein X-ray crystallography. *The FEBS Journal* **2021,** *288* (20), 5788-5804.
21. Edwards, G. B.; Muthurajan, U. M.; Bowerman, S.; Luger, K., Analytical Ultracentrifugation (AUC): An Overview of the Application of Fluorescence and Absorbance AUC to the Study of Biological Macromolecules. *Current Protocols in Molecular Biology* **2020,** *133* (1), e131.
22. Ebel, C., Sedimentation velocity to characterize surfactants and solubilized membrane proteins. *Methods* **2011,** *54* (1), 56-66.
23. Cole, J. L.; Lary, J. W.; T, P. M.; Laue, T. M., Analytical ultracentrifugation: sedimentation velocity and sedimentation equilibrium. *Methods Cell Biol* **2008,** *84*, 143-79.
24. Amartely, H.; Avraham, O.; Friedler, A.; Livnah, O.; Lebendiker, M., Coupling Multi Angle Light Scattering to Ion Exchange chromatography (IEX-MALS) for protein characterization. *Scientific Reports* **2018,** *8* (1), 6907.
25. Some, D.; Amartely, H.; Tsadok, A.; Lebendiker, M., Characterization of Proteins by Size-Exclusion Chromatography Coupled to Multi-Angle Light Scattering (SEC-MALS). *JoVE* **2019,** (148), e59615.

26. Wu, D.; Piszczek, G., Standard protocol for mass photometry experiments. *European Biophysics Journal* **2021,** *50* (3), 403-409.
27. Sonn-Segev, A.; Belacic, K.; Bodrug, T.; Young, G.; VanderLinden, R. T.; Schulman, B. A.; Schimpf, J.; Friedrich, T.; Dip, P. V.; Schwartz, T. U.; Bauer, B.; Peters, J. M.; Struwe, W. B.; Benesch, J. L. P.; Brown, N. G.; Haselbach, D.; Kukura, P., Quantifying the heterogeneity of macromolecular machines by mass photometry. *Nat Commun* **2020,** *11* (1), 1772.
28. Olerinyova, A.; Sonn-Segev, A.; Gault, J.; Eichmann, C.; Schimpf, J.; Kopf, A. H.; Rudden, L. S. P.; Ashkinadze, D.; Bomba, R.; Frey, L.; Greenwald, J.; Degiacomi, M. T.; Steinhilper, R.; Killian, J. A.; Friedrich, T.; Riek, R.; Struwe, W. B.; Kukura, P., Mass Photometry of Membrane Proteins. *Chem* **2021,** *7* (1), 224-236.
29. Wang, X.; Lee, H. W.; Liu, Y.; Prestegard, J. H., Structural NMR of protein oligomers using hybrid methods. *J Struct Biol* **2011,** *173* (3), 515-29.
30. Martin, J. W.; Yan, A. K.; Bailey-Kellogg, C.; Zhou, P.; Donald, B. R. In *A Geometric Arrangement Algorithm for Structure Determination of Symmetric Protein Homo-oligomers from NOEs and RDCs*, Research in Computational Molecular Biology, Berlin, Heidelberg, 2011//; Bafna, V.; Sahinalp, S. C., Eds. Springer Berlin Heidelberg: Berlin, Heidelberg, 2011; pp 222-237.
31. Sala, D.; Cerofolini, L.; Fragai, M.; Giachetti, A.; Luchinat, C.; Rosato, A., A protocol to automatically calculate homo-oligomeric protein structures through the integration of evolutionary constraints and NMR ambiguous contacts. *Computational and Structural Biotechnology Journal* **2020,** *18*, 114-124.
32. Luo, W.; Hong, M., Determination of the Oligomeric Number and Intermolecular Distances of Membrane Protein Assemblies by Anisotropic 1H-Driven Spin Diffusion NMR Spectroscopy. *Journal of the American Chemical Society* **2006,** *128* (22), 7242-7251.
33. Somberg, N. H.; Wu, W. W.; Medeiros-Silva, J.; Dregni, A. J.; Jo, H.; DeGrado, W. F.; Hong, M., SARS-CoV-2 Envelope Protein Forms Clustered Pentamers in Lipid Bilayers. *Biochemistry* **2022,** *61* (21), 2280-2294.
34. Yu, H., Extending the size limit of protein nuclear magnetic resonance. *Proceedings of the National Academy of Sciences* **1999,** *96* (2), 332-334.
35. Kozak, S.; Lercher, L.; Karanth, M. N.; Meijers, R.; Carlomagno, T.; Boivin, S., Optimization of protein samples for NMR using thermal shift assays. *J Biomol NMR* **2016,** *64* (4), 281-9.
36. Park, S. H.; Das, B. B.; De Angelis, A. A.; Scrima, M.; Opella, S. J., Mechanically, Magnetically, and "Rotationally Aligned" Membrane Proteins in Phospholipid Bilayers Give Equivalent Angular Constraints for NMR Structure Determination. *The Journal of Physical Chemistry B* **2010,** *114* (44), 13995-14003.
37. Gaber, A.; Gunčar, G.; Pavšič, M., Proper evaluation of chemical cross-linking-based spatial restraints improves the precision of modeling homo-oligomeric protein complexes. *BMC Bioinformatics* **2019,** *20* (1), 464.
38. Banerjee, R.; Günsel, U.; Mokranjac, D., Chemical Crosslinking in Intact Mitochondria. *Methods Mol Biol* **2017,** *1567*, 139-154.
39. Yang, B.; Tang, S.; Ma, C.; Li, S.-T.; Shao, G.-C.; Dang, B.; DeGrado, W. F.; Dong, M.-Q.; Wang, P. G.; Ding, S.; Wang, L., Spontaneous and specific chemical cross-linking in live cells to capture and identify protein interactions. *Nature Communications* **2017,** *8* (1), 2240.
40. Merkley, E. D.; Cort, J. R.; Adkins, J. N., Cross-linking and mass spectrometry methodologies to facilitate structural biology: finding a path through the maze. *J Struct Funct Genomics* **2013,** *14* (3), 77-90.
41. Wang, Z.; Lu, W.; Rajapaksha, P.; Wilkop, T.; Cai, Y.; Wei, Y., Comparison of in vitro and in vivo oligomeric states of a wild type and mutant trimeric inner membrane multidrug transporter. *Biochem Biophys Rep* **2018,** *16*, 122-129.

42. Muzzopappa, F.; Hummert, J.; Anfossi, M.; Tashev, S. A.; Herten, D.-P.; Erdel, F., Detecting and quantifying liquid–liquid phase separation in living cells by model-free calibrated half-bleaching. *Nature Communications* **2022,** *13* (1), 7787.
43. Weiss, M., Challenges and artifacts in quantitative photobleaching experiments. *Traffic* **2004,** *5* (9), 662-71.
44. Barth, M.; Schmidt, C., Native mass spectrometry—A valuable tool in structural biology. *Journal of Mass Spectrometry* **2020,** *55* (10), e4578.
45. Heuvel, R. H. H. v. d.; Heck, A. J. R., Native protein mass spectrometry: from intact oligomers to functional machineries. *Current Opinion in Chemical Biology* **2004,** *8* (5), 519-526.
46. Keener, J. E.; Zhang, G.; Marty, M. T., Native Mass Spectrometry of Membrane Proteins. *Analytical Chemistry* **2021,** *93* (1), 583-597.
47. Leney, A. C.; Heck, A. J. R., Native Mass Spectrometry: What is in the Name? *J Am Soc Mass Spectrom* **2017,** *28* (1), 5-13.
48. Urban, P. L., Quantitative mass spectrometry: an overview. *Philos Trans A Math Phys Eng Sci* **2016,** *374* (2079).
49. Bui, D. T.; Li, Z.; Kitov, P. I.; Han, L.; Kitova, E. N.; Fortier, M.; Fuselier, C.; Granger Joly de Boissel, P.; Chatenet, D.; Doucet, N.; Tompkins, S. M.; St-Pierre, Y.; Mahal, L. K.; Klassen, J. S., Quantifying Biomolecular Interactions Using Slow Mixing Mode (SLOMO) Nanoflow ESI-MS. *ACS Cent Sci* **2022,** *8* (7), 963-974.
50. Marty, M. T., Nanodiscs and mass spectrometry: Making membranes fly. *International Journal of Mass Spectrometry* **2020,** *458*, 116436.
51. Gault, J.; Donlan, J. A. C.; Liko, I.; Hopper, J. T. S.; Gupta, K.; Housden, N. G.; Struwe, W. B.; Marty, M. T.; Mize, T.; Bechara, C.; Zhu, Y.; Wu, B.; Kleanthous, C.; Belov, M.; Damoc, E.; Makarov, A.; Robinson, C. V., High-resolution mass spectrometry of small molecules bound to membrane proteins. *Nature Methods* **2016,** *13* (4), 333-336.
52. Zhou, M.; Morgner, N.; Barrera, N. P.; Politis, A.; Isaacson, S. C.; Matak-Vinković, D.; Murata, T.; Bernal, R. A.; Stock, D.; Robinson, C. V., Mass spectrometry of intact V-type ATPases reveals bound lipids and the effects of nucleotide binding. *Science* **2011,** *334* (6054), 380-385.
53. Sahin, C.; Reid, D. J.; Marty, M. T.; Landreh, M., Scratching the surface: native mass spectrometry of peripheral membrane protein complexes. *Biochem Soc Trans* **2020,** *48* (2), 547-558.
54. Hellwig, N.; Peetz, O.; Ahdash, Z.; Tascón, I.; Booth, P. J.; Mikusevic, V.; Diskowski, M.; Politis, A.; Hellmich, Y.; Hänelt, I.; Reading, E.; Morgner, N., Native mass spectrometry goes more native: investigation of membrane protein complexes directly from SMALPs. *Chemical Communications* **2018,** *54* (97), 13702-13705.
55. Frick, M.; Schwieger, C.; Schmidt, C., Liposomes as Carriers of Membrane-Associated Proteins and Peptides for Mass Spectrometric Analysis. *Angewandte Chemie International Edition* **2021,** *60* (20), 11523-11530.
56. Marty, M. T.; Hoi, K. K.; Robinson, C. V., Interfacing Membrane Mimetics with Mass Spectrometry. *Accounts of Chemical Research* **2016,** *49* (11), 2459-2467.
57. Denisov, I. G.; Sligar, S. G., Nanodiscs for structural and functional studies of membrane proteins. *Nature Structural & Molecular Biology* **2016,** *23* (6), 481-486.
58. Wang, X.; Mu, Z.; Li, Y.; Bi, Y.; Wang, Y., Smaller Nanodiscs are Suitable for Studying Protein Lipid Interactions by Solution NMR. *The Protein Journal* **2015,** *34* (3), 205-211.
59. Padmanabha Das, K. M.; Shih, W. M.; Wagner, G.; Nasr, M. L., Large Nanodiscs: A Potential Game Changer in Structural Biology of Membrane Protein Complexes and Virus Entry. *Front Bioeng Biotechnol* **2020,** *8*, 539.
60. Sligar, S. G.; Denisov, I. G., Nanodiscs: A toolkit for membrane protein science. *Protein Science* **2021,** *30* (2), 297-315.

61. Borch, J.; Hamann, T., The nanodisc: a novel tool for membrane protein studies. *Biol Chem* **2009,** *390* (8), 805-14.
62. Botelho, A. V.; Huber, T.; Sakmar, T. P.; Brown, M. F., Curvature and Hydrophobic Forces Drive Oligomerization and Modulate Activity of Rhodopsin in Membranes. *Biophys J* **2006,** *91* (12), 4464-4477.
63. Gupta, K.; Donlan, J. A. C.; Hopper, J. T. S.; Uzdavinys, P.; Landreh, M.; Struwe, W. B.; Drew, D.; Baldwin, A. J.; Stansfeld, P. J.; Robinson, C. V., The role of interfacial lipids in stabilizing membrane protein oligomers. *Nature* **2017,** *541* (7637), 421-424.
64. Marty, M. T.; Zhang, H.; Cui, W.; Blankenship, R. E.; Gross, M. L.; Sligar, S. G., Native Mass Spectrometry Characterization of Intact Nanodisc Lipoprotein Complexes. *Analytical Chemistry* **2012,** *84* (21), 8957-8960.
65. Keener, J. E.; Zambrano, D. E.; Zhang, G.; Zak, C. K.; Reid, D. J.; Deodhar, B. S.; Pemberton, J. E.; Prell, J. S.; Marty, M. T., Chemical Additives Enable Native Mass Spectrometry Measurement of Membrane Protein Oligomeric State within Intact Nanodiscs. *Journal of the American Chemical Society* **2019,** *141* (2), 1054-1061.
66. Marty, M. T.; Baldwin, A. J.; Marklund, E. G.; Hochberg, G. K. A.; Benesch, J. L. P.; Robinson, C. V., Bayesian Deconvolution of Mass and Ion Mobility Spectra: From Binary Interactions to Polydisperse Ensembles. *Analytical Chemistry* **2015,** *87* (8), 4370-4376.
67. Denisov, I. G.; Grinkova, Y. V.; Lazarides, A. A.; Sligar, S. G., Directed Self-Assembly of Monodisperse Phospholipid Bilayer Nanodiscs with Controlled Size. *Journal of the American Chemical Society* **2004,** *126* (11), 3477-3487.
68. Reid, D. J.; Rohrbough, J. G.; Kostelic, M. M.; Marty, M. T., Investigating Antimicrobial Peptide–Membrane Interactions Using Fast Photochemical Oxidation of Peptides in Nanodiscs. *J Am Soc Mass Spectrom* **2022,** *33* (1), 62-67.
69. Reid, D. J.; Keener, J. E.; Wheeler, A. P.; Zambrano, D. E.; Diesing, J. M.; Reinhardt-Szyba, M.; Makarov, A.; Marty, M. T., Engineering Nanodisc Scaffold Proteins for Native Mass Spectrometry. *Analytical Chemistry* **2017,** *89* (21), 11189-11192.
70. Marty, M. T.; Hoi, K. K.; Gault, J.; Robinson, C. V., Probing the Lipid Annular Belt by Gas-Phase Dissociation of Membrane Proteins in Nanodiscs. *Angewandte Chemie International Edition* **2016,** *55* (2), 550-554.
71. Roach, P. J.; Laskin, J.; Laskin, A., Higher-Order Mass Defect Analysis for Mass Spectra of Complex Organic Mixtures. *Analytical Chemistry* **2011,** *83* (12), 4924-4929.
72. Swansiger, A. K.; Marty, M. T.; Prell, J. S., Fourier-Transform Approach for Reconstructing Macromolecular Mass Defect Profiles. *J Am Soc Mass Spectrom* **2022,** *33* (1), 172-180.
73. Fouquet, T. N. J., The Kendrick analysis for polymer mass spectrometry. *Journal of Mass Spectrometry* **2019,** *54* (12), 933-947.
74. Kendrick, E., A Mass Scale Based on CH2 = 14.0000 for High Resolution Mass Spectrometry of Organic Compounds. *Analytical Chemistry* **1963,** *35* (13), 2146-2154.
75. Walker, L. R.; Marzluff, E. M.; Townsend, J. A.; Resager, W. C.; Marty, M. T., Native Mass Spectrometry of Antimicrobial Peptides in Lipid Nanodiscs Elucidates Complex Assembly. *Analytical Chemistry* **2019,** *91* (14), 9284-9291.
76. Lerno, L. A., Jr.; German, J. B.; Lebrilla, C. B., Method for the identification of lipid classes based on referenced Kendrick mass analysis. *Anal Chem* **2010,** *82* (10), 4236-45.
77. Hustin, J.; Kune, C.; Far, J.; Eppe, G.; Debois, D.; Quinton, L.; De Pauw, E., Differential Kendrick's Plots as an Innovative Tool for Lipidomics in Complex Samples: Comparison of Liquid Chromatography and Infusion-Based Methods to Sample Differential Study. *J Am Soc Mass Spectrom* **2022,** *33* (12), 2273-2282.
78. Sleno, L., The use of mass defect in modern mass spectrometry. *Journal of Mass Spectrometry* **2012,** *47* (2), 226-236.

79. Zubarev, R. A.; Makarov, A., Orbitrap Mass Spectrometry. *Analytical Chemistry* **2013,** *85* (11), 5288-5296.
80. Kostelic, M. M.; Zak, C. K.; Jayasekera, H. S.; Marty, M. T., Assembly of Model Membrane Nanodiscs for Native Mass Spectrometry. *Analytical Chemistry* **2021,** *93* (14), 5972-5979.
81. Cleary, S. P.; Prell, J. S., Liberating Native Mass Spectrometry from Dependence on Volatile Salt Buffers by Use of Gábor Transform. *ChemPhysChem* **2019,** *20* (4), 519-523.
82. Walker, L. R.; Marty, M. T., Revealing the Specificity of a Range of Antimicrobial Peptides in Lipid Nanodiscs by Native Mass Spectrometry. *Biochemistry* **2020,** *59* (23), 2135-2142.
83. Walker, L. R.; Marty, M. T., Lipid tails modulate antimicrobial peptide membrane incorporation and activity. *Biochimica et Biophysica Acta (BBA) - Biomembranes* **2022,** *1864* (4), 183870.
84. LaPlante Kerry, L.; Woodmansee, S., Activities of Daptomycin and Vancomycin Alone and in Combination with Rifampin and Gentamicin against Biofilm-Forming Methicillin-Resistant Staphylococcus aureus Isolates in an Experimental Model of Endocarditis. *Antimicrobial Agents and Chemotherapy* **2009,** *53* (9), 3880-3886.
85. Rose, W. E.; Leonard, S. N.; Sakoulas, G.; Kaatz, G. W.; Zervos, M. J.; Sheth, A.; Carpenter, C. F.; Rybak, M. J., daptomycin activity against Staphylococcus aureus following vancomycin exposure in an in vitro pharmacodynamic model with simulated endocardial vegetations. *Antimicrob Agents Chemother* **2008,** *52* (3), 831-6.
86. Johnson, A. R.; Carlson, E. E., Collision-Induced Dissociation Mass Spectrometry: A Powerful Tool for Natural Product Structure Elucidation. *Analytical Chemistry* **2015,** *87* (21), 10668-10678.
87. Zhang, G.; Keener, J. E.; Marty, M. T., Measuring Remodeling of the Lipid Environment Surrounding Membrane Proteins with Lipid Exchange and Native Mass Spectrometry. *Anal Chem* **2020,** *92* (8), 5666-5669.
88. Sanders, H. M.; Kostelic, M. M.; Zak, C. K.; Marty, M. T., Lipids and EGCG Affect α-Synuclein Association and Disruption of Nanodiscs. *Biochemistry* **2022,** *61* (11), 1014-1021.
89. Townsend, J. A.; Sanders, H. M.; Rolland, A. D.; Park, C. K.; Horton, N. C.; Prell, J. S.; Wang, J.; Marty, M. T., Influenza AM2 Channel Oligomerization Is Sensitive to Its Chemical Environment. *Analytical Chemistry* **2021,** *93* (48), 16273-16281.
90. Gevaert, K.; Impens, F.; Ghesquière, B.; Van Damme, P.; Lambrechts, A.; Vandekerckhove, J., Stable isotopic labeling in proteomics. *Proteomics* **2008,** *8* (23-24), 4873-85.
91. Johnson, D. T.; Di Stefano, L. H.; Jones, L. M., Fast photochemical oxidation of proteins (FPOP): A powerful mass spectrometry-based structural proteomics tool. *J Biol Chem* **2019,** *294* (32), 11969-11979.
92. Konermann, L.; Pan, J.; Liu, Y. H., Hydrogen exchange mass spectrometry for studying protein structure and dynamics. *Chem Soc Rev* **2011,** *40* (3), 1224-34.
93. Reid Deseree, D. T., Wang Zhihan, Aspinwall Craig, Marty Michael., Daptomycin-Membrane Interactions Using Native MS and Fast Photochemical Oxidation of Peptides in Nanodiscs. *ChemRxiv* **2022**.
94. Sanders, H.; Chalyavi, F.; Fields, C.; Kostelic, M. M.; Li, M.-H.; Raleigh, D.; Zanni, M.; Marty, M. T., Interspecies Variation Affects IAPP Membrane Binding. *ChemRxiv* **2023**.
95. Kaldmäe, M.; Österlund, N.; Lianoudaki, D.; Sahin, C.; Bergman, P.; Nyman, T.; Kronqvist, N.; Ilag, L. L.; Allison, T. M.; Marklund, E. G.; Landreh, M., Gas-Phase Collisions with Trimethylamine-N-Oxide Enable Activation-Controlled Protein Ion Charge Reduction. *J Am Soc Mass Spectrom* **2019,** *30* (8), 1385-1388.
96. Townsend, J. A.; Keener, J. E.; Miller, Z. M.; Prell, J. S.; Marty, M. T., Imidazole Derivatives Improve Charge Reduction and Stabilization for Native Mass Spectrometry. *Analytical Chemistry* **2019,** *91* (22), 14765-14772.

97. Pacholarz, K. J.; Barran, P. E., Use of a charge reducing agent to enable intact mass analysis of cysteine-linked antibody-drug-conjugates by native mass spectrometry. *EuPA Open Proteomics* **2016,** *11*, 23-27.
98. Jiang, J.; Daniels, B. V.; Fu, D., Crystal Structure of AqpZ Tetramer Reveals Two Distinct Arg-189 Conformations Associated with Water Permeation through the Narrowest Constriction of the Water-conducting Channel*. *Journal of Biological Chemistry* **2006,** *281* (1), 454-460.
99. Ringler, P.; Borgnia, M. J.; Stahlberg, H.; Maloney, P. C.; Agre, P.; Engel, A., Structure of the water channel AqpZ from Escherichia coli revealed by electron crystallography. *J Mol Biol* **1999,** *291* (5), 1181-90.
100. Epand, R. M.; Epand, R. F., Lipid domains in bacterial membranes and the action of antimicrobial agents. *Biochimica et Biophysica Acta (BBA) - Biomembranes* **2009,** *1788* (1), 289-294.
101. Savini, F.; Loffredo, M. R.; Troiano, C.; Bobone, S.; Malanovic, N.; Eichmann, T. O.; Caprio, L.; Canale, V. C.; Park, Y.; Mangoni, M. L.; Stella, L., Binding of an antimicrobial peptide to bacterial cells: Interaction with different species, strains and cellular components. *Biochimica et Biophysica Acta (BBA) - Biomembranes* **2020,** *1862* (8), 183291.
102. Mondal, S.; Khelashvili, G.; Weinstein, H., Not Just an Oil Slick: How the Energetics of Protein-Membrane Interactions Impacts the Function and Organization of Transmembrane Proteins. *Biophys J* **2014,** *106* (11), 2305-2316.
103. Bieschke, J.; Russ, J.; Friedrich, R. P.; Ehrnhoefer, D. E.; Wobst, H.; Neugebauer, K.; Wanker, E. E., EGCG remodels mature alpha-synuclein and amyloid-beta fibrils and reduces cellular toxicity. *Proc Natl Acad Sci U S A* **2010,** *107* (17), 7710-5.
104. Fernandes, L.; Cardim-Pires, T. R.; Foguel, D.; Palhano, F. L., Green Tea Polyphenol Epigallocatechin-Gallate in Amyloid Aggregation and Neurodegenerative Diseases. *Front Neurosci* **2021,** *15*, 718188.
105. Cady, S. D.; Hong, M., Amantadine-induced conformational and dynamical changes of the influenza M2 transmembrane proton channel. *Proceedings of the National Academy of Sciences* **2008,** *105* (5), 1483-1488.
106. Cady, S. D.; Schmidt-Rohr, K.; Wang, J.; Soto, C. S.; DeGrado, W. F.; Hong, M., Structure of the amantadine binding site of influenza M2 proton channels in lipid bilayers. *Nature* **2010,** *463* (7281), 689-692.
107. Schnell, J. R.; Chou, J. J., Structure and mechanism of the M2 proton channel of influenza A virus. *Nature* **2008,** *451* (7178), 591-595.
108. Thomaston, J. L.; Polizzi, N. F.; Konstantinidi, A.; Wang, J.; Kolocouris, A.; DeGrado, W. F., Inhibitors of the M2 Proton Channel Engage and Disrupt Transmembrane Networks of Hydrogen-Bonded Waters. *Journal of the American Chemical Society* **2018,** *140* (45), 15219-15226.
109. Keating, A. R.; Wesdemiotis, C., Rapid and simple determination of average molecular weight and composition of synthetic polymers via electrospray ionization-mass spectrometry and a Bayesian universal charge deconvolution. *Rapid Communications in Mass Spectrometry* **2023,** *37* (8), e9478.
110. Wu, D.; Li, J.; Struwe, W. B.; Robinson, Carol V., Probing N-glycoprotein microheterogeneity by lectin affinity purification-mass spectrometry analysis. *Chemical Science* **2019,** *10* (19), 5146-5155.
111. Wu, D.; Struwe, W. B.; Harvey, D. J.; Ferguson, M. A. J.; Robinson, C. V., N-glycan microheterogeneity regulates interactions of plasma proteins. *Proceedings of the National Academy of Sciences* **2018,** *115* (35), 8763-8768.